# Nonlinear transmission properties of hydrogenated amorphous silicon core fibers towards the mid-infrared regime

**L. Shen,[1] N. Healy,[1] P. Mehta,[1] T. D. Day,[2] J. R. Sparks,[2] J. V. Badding,[2] and A. C. Peacock[1,*]**

*1. Optoelectronics Research Centre, University of Southampton, Southampton SO17 1BJ, UK*
*2. Department of Chemistry and Materials Research Institute, Pennsylvania State University 16802 PA, USA*

*[*]acp@orc.soton.ac.uk*

**Abstract:** The nonlinear transmission properties of hydrogenated amorphous silicon (a-Si:H) core fibers are characterized from the near-infrared up to the edge of the mid-infrared regime. The results show that this material exhibits linear losses on the order of a few dB/cm, or less, over the entire wavelength range, decreasing down to a value of 0.29 dB/cm at 2.7 $\mu$m, and negligible nonlinear losses beyond the two-photon absorption (TPA) edge $\sim 1.7\,\mu$m. By measuring the dispersion of the nonlinear Kerr and TPA parameters we have found that the nonlinear figure of merit ($FOM_{NL}$) increases dramatically over this region, with $FOM_{NL} > 20$ around 2 $\mu$m and above. This characterization demonstrates the potential for a-Si:H fibers and waveguides to find use in nonlinear applications extending beyond telecoms and into the mid-infrared regime.



**OCIS codes:** (060.2270) Fiber characterization; (060.2290) Fiber materials; (060.4370) Nonlinear optics, fibers.

## References and links

1. K. Narayanan and S. F. Preble, "Optical nonlinearities in hydrogenated-amorphous silicon waveguides," Opt. Express **18**, 8998–9005 (2010).
2. C. Grillet, L. Carletti, C. Monat, P. Grosse, B. Ben Bakir, S. Menezo, J. M. Fedeli, and D. J. Moss, "Amorphous silicon nanowires combining high nonlinearity, FOM and optical stability," Opt. Express **20**, 22609–22615 (2012).
3. B. Kuyken, H. Ji, S. Clemmen, S. K. Selvaraja, H. Hu, M. Pu, M. Galili, P. Jeppesen, G. Morthier, S. Massar, L. K. Oxenløwe, G. Roelkens, and R. Baets, "Nonlinear properties of and nonlinear processing in hydrogenated amorphous silicon waveguides," Opt. Express **19**, B146–B153 (2011).
4. P. Mehta, N. Healy, N. F. Baril, P. J. A. Sazio, J. V. Badding, and A. C. Peacock, "Nonlinear transmission properties of hydrogenated amorphous silicon core optical fibers," Opt. Express **18**, 16826–16831 (2010).
5. K. Narayanan, A. W. Elshaari, and S. F. Preble, "Broadband all-optical modulation in hydrogenated-amorphous silicon waveguides," Opt. Express **18**, 9809–9814 (2010).
6. P. Mehta, N. Healy, T. D. Day, J. R. Sparks, P. J. A. Sazio, J. V. Badding, and A. C. Peacock, "All-optical modulation using two-photon absorption in silicon core optical fibers," Opt. Express **19**, 19078–19083 (2011).
7. S. Clemmen, A. Perret, S. K. Selvaraja, W. Bogaerts, D. van Thourhout, R. Baets, Ph. Emplit, and S. Massar, "Generation of correlated photons in hydrogenated amorphous-silicon waveguides," Opt. Lett. **35**, 3483–3485 (2010).
8. B. Kuyken, S. Clemmen, S. K. Selvaraja, W. Bogaerts, D. Van Thourhout, Ph. Emplit, S. Massar, G. Roelkens, and R. Baets, "On-chip parametric amplification with 26.5 dB gain at telecommunication wavelengths using CMOS-compatible hydrogenated amorphous silicon waveguides," Opt. Lett. **36**, 552–554 (2011).

#188410 - $15.00 USD Received 5 Apr 2013; revised 3 May 2013; accepted 13 May 2013; published 21 May 2013

9. K.-Y. Wang and A. C. Foster, "Ultralow power continuous-wave frequency conversion in hydrogenated amorphous silicon waveguides," Opt. Lett. **37**, 1331–1333 (2012).
10. B. Kuyken, X. Liu, G. Roelkens, R. Baets, R. M. Osgood, Jr., and W. M. J. Green, "50 dB parametric on-chip gain in silicon photonic wires," Opt. Lett. **36**, 4401–4403 (2011).
11. B. Kuyken, X. Liu, R. M. Osgood Jr., R. Baets, G. Roelkens, and W. M. J. Green, "Mid-infrared to telecom-band supercontinuum generation in highly nonlinear silicon-on-insulator wire waveguides," Opt. Express **19**, 20172–20181 (2011).
12. N. F. Baril, R. He, Rongrui, T. D. Day, J. R. Sparks, B. Keshavarzi, M. Krishnamurthi, A. Borhan, V. Gopalan, A. C. Peacock, N. Healy, P. J. A. Sazio, and J. V. Badding, "Confined high-pressure chemical deposition of hydrogenated amorphous silicon," J. Am. Chem. Soc. **134**, 19–22 (2011).
13. J. Ballato, T. Hawkins, P. Foy, B. Yazgan-Kokuoz, C. McMillen, L. Burka, S. Morris, R. Stolen, and R. Rice, "Advancements in semiconductor core optical fiber," Opt. Fiber Technol. **16**, 399–408 (2010).
14. P. Mehta, N. Healy, T. D. Day, J. V. Badding, and A. C. Peacock, "Ultrafast wavelength conversion via cross-phase modulation in hydrogenated amorphous silicon optical fibers," Opt. Express **20**, 26110–26116 (2012).
15. N. Healy, J. R. Sparks, P. J. A. Sazio, J. V. Badding, and A. C. Peacock, "Tapered silicon optical fibers," Opt. Express **18**, 7596–7601 (2010).
16. L. Yin and G. P. Agrawal, "Impact of two-photon absorption on self-phase modulation in silicon waveguides," Opt. Lett. **32**, 2031–2033 (2007).
17. H. H. Li, "Refractive index of silicon and germanium and its wavelength and temperature derivatives," J. Phys. Chem. Ref. Data **9**, 561–658 (1980).
18. J. Matres, G. C. Ballesteros, P. Gautier, J.-M. Fédéli, J. Martí, and C. J. Oton, "High nonlinear figure-of-merit amorphous silicon waveguides," Opt. Express **21**, 3932–3940 (2013).
19. A. C. Peacock, P. Mehta, P. Horak, and N. Healy, "Nonlinear pulse dynamics in multimode silicon core optical fibers," Opt. Lett. **37**, 3351–3353 (2012).
20. L. Lagonigro, N. Healy, J. R. Sparks, N. F. Baril, P. J. A. Sazio, J. V. Badding, and A. C. Peacock, "Low loss silicon fibers for photonics applications," Appl. Phys. Lett. **96**, 041105 (2010).
21. S. K. Selvaraja, E. Sleeckx, M. Schaekers, W. Bogaerts, D. Van Thourhout, P. Dumon, and R. Baets, "Low-loss amorphous silicon-on-insulator technology for photonic integrated circuitry," Opt. Commun. **282**, 1767–1770 (2009).
22. Y. Shoji, T. Ogasawara, T. Kamei, Y. Sakakibara, S. Suda, K. Kintaka, H. Kawashima, M. Okano, T. Hasama, H. Ishikawa, and M. Mori, "Ultrafast nonlinear effects in hydrogenated amorphous silicon wire waveguide," Opt. Express **18**, 5668–5673 (2010).
23. J. S. Sanghera, I. D. Aggarwal, L. B. Shaw, C. M. Florea, P. Pureza, V. Q. Nguyen, F. Kung, and I. D. Aggarwal, "Nonlinear properties of chalcogenide glass fibers," J. Optoelectron. Adv. M. **8**, 2148–2155 (2006).
24. A. D. Bristow, N. Rotenberg, and H. M. Van Driel,"Two-photon absorption and Kerr coefficients of silicon for 850 – 2200 nm," Appl. Phys. Lett. **90**, 191104 (2007).

## 1. Introduction

Hydrogenated amorphous silicon (a-Si:H) is becoming an increasingly popular material for nonlinear silicon photonics due to its low transmission losses, high Kerr nonlinear coefficient $n_2$, and low fabrication costs [1]. In addition, compared to crystalline silicon (c-Si), a-Si:H also has a larger bandgap energy ($E_g \sim 1.7\,\text{eV}$), which suggests that the nonlinear absorption should be modest at telecoms wavelengths that are past the two-photon absorption (TPA) edge. However, in practice the values of the TPA parameter $\beta_{\text{TPA}}$ measured around $1.5\,\mu\text{m}$ vary quite substantially, usually attributed to differences in the fabrication methods, with some groups reporting values that are lower than c-Si [2], but most reporting values that are of a comparable size [1, 3]. Despite these variations in $\beta_{\text{TPA}}$, the consistently higher values of $n_2$ of the a-Si:H material typically results in considerably larger values of the nonlinear figure of merit $\text{FOM}_{\text{NL}} = n_2/\beta_{\text{TPA}}\lambda$ [1, 3, 4]. Thus, to date, a number of important photonic functions have been demonstrated in a-Si:H waveguides in the near-infrared wavelength region including all-optical modulation [5, 6], photon pair generation [7], and parametric amplification [8, 9]. Although it should be possible to achieve even higher values of the $\text{FOM}_{\text{NL}}$ at longer wavelengths where TPA becomes negligible, there has yet to be any systematic studies of the wavelength dependence of $n_2$ and $\beta_{\text{TPA}}$ in a-Si:H. In contrast, studies in c-Si have recently shown that by operating past the TPA edge, very high parametric gains (over 50 dB) [10] and broadband supercontinuum [11] can be achieved.

#188410 - $15.00 USD Received 5 Apr 2013; revised 3 May 2013; accepted 13 May 2013; published 21 May 2013

In complement to the research that is currently being undertaken on-chip, we have been investigating a new class of a-Si:H core optical fiber that is fabricated using a high pressure chemical vapour deposition (HPCVD) method [12]. This method differs from the plasma enhanced CVD technique used for the fabrication of the on-chip waveguides, particularly in terms of the way that the hydrogen is incorporated, yet the resulting materials have similar nonlinear parameters [2, 4]. In addition, unlike some reports on-chip [3], these a-Si:H fibers have exhibited excellent stability over several months of use, for input peak powers of hundreds of watts. Briefly, the deposition process is conducted by forcing a mixture of precursor gas (silane $SiH_4$ and hydrogen $H_2$) to flow through a silica capillary under high pressures ($2-100\,\mathrm{MPa}$), at temperatures between $360-440\,^{\circ}\mathrm{C}$. The high pressures increase the deposition rate at the low temperatures, which leads to incorporation of hydrogen via the incomplete decomposition of silane to silicon. The ability to incorporate amorphous semiconductor materials into the fiber geometry is a direct consequence of this low temperature deposition, and alternative high temperature fiber drawing methods have so far only been used to produce crystalline semiconductor core fibers [13]. We have previously reported on the nonlinear optical properties and the associated $\mathrm{FOM_{NL}}$ of these a-Si:H fibers at the telecoms wavelength of $1.54\,\mu\mathrm{m}$, and by exploiting the ultrafast $\beta_{\mathrm{TPA}}$ and large $n_2$, demonstrated all-optical modulation and wavelength switching schemes [6, 14]. These silicon-based fibers provide an important step towards integrating semiconductor functionality with conventional fiber infrastructures as well as allowing for the construction of robust devices with novel waveguiding properties [15].

In this paper, we extend the characterization of our a-Si:H core fibers beyond the telecommunications window, and present the first measurements of the transmission properties of this promising material up to the mid-infrared (mid-IR) regime. A series of wavelength dependent measurements spanning $\sim 1.5-2.3\,\mu\mathrm{m}$ have been conducted using various continuous wave and short pulse laser sources to determine both the linear losses and the nonlinear transmission properties related to the $\beta_{\mathrm{TPA}}$ and $n_2$ coefficients. This characterization provides useful information regarding the dispersion of the $\mathrm{FOM_{NL}}$ in the vicinity of the TPA edge. The combination of the lower linear losses ($\lesssim 1\,\mathrm{dB/cm}$) and the negligible nonlinear absorption for wavelengths $> 1.7\,\mu\mathrm{m}$ indicate the potential for these a-Si:H fibers to find use for nonlinear applications in areas such as broadband and/or free-space communications, as well as some mid-IR gas sensing and medical applications.

## 2. Pulse propagation in a silicon optical fiber

The propagation of optical pulses in silicon core fibers can be described using a generalized form of the nonlinear Schrödinger equation (NLSE) that has been modified to account for the effects of TPA, and the TPA induced free carriers [16]:

$$\frac{\partial A(z,t)}{\partial z} = -\frac{i\beta_2}{2}\frac{\partial^2 A(z,t)}{\partial t^2} + i\gamma|A(z,t)|^2 A(z,t) - \frac{1}{2}(\alpha_l + \sigma_f)A(z,t). \tag{1}$$

Here $A(z,t)$, $\beta_2$, $\gamma$, $\alpha_l$, and $\sigma_f$ represent the slowly varying pulse envelope, group velocity dispersion (GVD), nonlinear parameter, linear loss, and the free carrier contribution, respectively. A complex nonlinear parameter is included to account for both the Kerr and TPA contributions: $\gamma = k_0 n_2/A_{\mathrm{eff}} + i\beta_{\mathrm{TPA}}/2A_{\mathrm{eff}}$, where $A_{\mathrm{eff}}$ is the mode area. Similarly, the free carrier contribution is also complex: $\sigma_f = \sigma(1+i\mu)N_c$, where $\sigma$ is the free carrier absorption (FCA) coefficient and $\mu$ governs the free-carrier dispersion (FCD). The free carrier density $N_c$ is related to the TPA parameter and can be determined via the rate equation [16]:

$$\frac{\partial N_c(z,t)}{\partial t} = \frac{\beta_{\mathrm{TPA}}}{2h\nu_0}\frac{|A(z,t)|^4}{A_{\mathrm{eff}}^2} - \frac{N_c(z,t)}{\tau_c}, \tag{2}$$

#188410 - $15.00 USD Received 5 Apr 2013; revised 3 May 2013; accepted 13 May 2013; published 21 May 2013

where $\tau_c$ is the carrier life time.

The aim of our investigations is to determine the wavelength dependence of $\alpha_l$, $\beta_{\mathrm{TPA}}$, and $n_2$. As the material dispersion for a-Si:H is not well documented, we approximate this using the Sellmeier equation for c-Si [17], and estimate $\beta_2(\lambda)$ using finite element methods (FEM). The validity of this assumption is supported by previous work which has shown that these simulations are in reasonable agreement with interferometric measurements [18]. Furthermore, for the nonlinear absorption measurements we use fiber lengths that are much shorter than the dispersion length $L_{\mathrm{D}} = T_0^2/|\beta_2|$, and for the Kerr measurements we use high peak power pulses so that the nonlinear effects dominate, i.e., $L_{\mathrm{NL}} = 1/\gamma P_0 \ll L_{\mathrm{D}}$.

## 3. Characterization of the optical transmission properties

### *3.1. Experimental configuration*

Our optical characterizations are based on transmission measurements in a 2.4 cm long a-Si:H fiber with a core diameter of $5.7\,\mu$m, that are conducted using the experimental setup shown in Fig. 1(a). Different laser sources were employed to measure both the linear losses and nonlinear parameters over the broad wavelength range $1.45-2.3\,\mu$m, and will be described separately for each measurement. A variable attenuator was used to control the power coupled into the fiber from the different sources to access the high and low power regimes. The light was launched into the fiber core via free space coupling using a $40\times$ magnification microscope objective lens, and a second $40\times$ objective was used to capture the transmitted light and focus it onto a lead selenide (PbSe) detector or an optical spectrum analyzer (OSA). Two beam splitters $(90/10)$ were placed before and after the fiber to capture, firstly, the reflected light from the input end face, and, secondly, the transmitted light from the output end face, which were monitored using two CCD cameras (CCD1 and CCD2). The use of these cameras ensured efficient coupling into the center of the core so that the fundamental mode was primarily excited [19].

### *3.2. Linear propagation loss*

The linear loss measurements were undertaken with two laser sources: (i) a Ti:sappire pumped femtosecond optical parametric oscillator (OPO) for the near-IR measurements spanning $1.45-2\,\mu$m and (ii) a continuous wave (CW) tunable $Cr^{2+}:ZnSe$ laser which covered the mid-IR wavelengths of $2-2.3\,\mu$m, as shown in Fig. 1(a). The input and output powers were

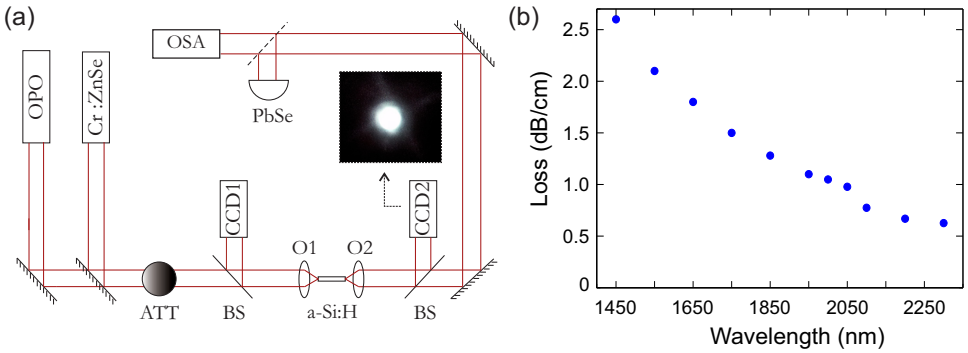


Fig. 1. (a) Schematic of the transmission setup. Attenuator (ATT), beam-splitter (BS), microscope objective lenses (O1 & O2), CCD detectors (CCD1 & CCD2), PbSe detector, optical spectrum analyser (OSA). Inset is the guided beam imaged on CCD2. (b) Linear loss measurements as a function of wavelength.

#188410 - $15.00 USD Received 5 Apr 2013; revised 3 May 2013; accepted 13 May 2013; published 21 May 2013

both monitored using power meters. In order to avoid the effects of nonlinear absorption when using the OPO, which had a pulse duration of 200 fs (FWHM) and a repetition rate of 80 MHz, the average launch power was kept below 100 $\mu$W. The losses were then determined using the cutback method, during which several sections were cut from the fiber so that the total removed length was 1.1 cm. The loss values over the entire wavelength range are shown in Fig. 1(b). These results follow the same trend of decreasing loss for increasing wavelength observed in earlier measurements of the silicon core fibers [20], and in this amorphous material the main contributions to the losses are likely to be a combination of scattering due to density fluctuations and some electronic absorption. These losses are some of the lowest reported for a-Si:H waveguides that are usually within the range: $1-10\,\mathrm{dB/cm}$ at telecoms wavelengths [21, 22], and the value of $2.1\,\mathrm{dB/cm}$ at $1.55\,\mu$m is the lowest we have measured in a a-Si:H fiber of several centimeters in length. To verify this value, additional measurements were conducted with a $1.55\,\mu$m CW diode, which returned the same loss, confirming that the nonlinear absorption was indeed negligible for the results taken with the OPO. Moreover, the losses in the range $2-2.3\,\mu$m are the first reported for this material in the mid-IR regime, and are all $\lesssim 1\,\mathrm{dB/cm}$, reducing to $0.62\,\mathrm{dB/cm}$ at $2.3\,\mu$m. Additional measurements undertaken at $2.7\,\mu$m (the limit of the $Cr^{2+}$ : ZnSe laser) revealed that the losses continued to decrease down to $0.29\,\mathrm{dB/cm}$. We expect that the losses across the entire wavelength region could be reduced even further by improving the hydrogenation during the deposition, both in terms of concentration and uniformity, and this is a focus of our ongoing materials work.

### *3.3. Nonlinear absorption across the TPA edge*

As the precise position of the TPA edge is not known for our a-Si:H material, we investigated the role of TPA for a range of wavelengths spanning half the theoretical bandgap energy of a-Si:H ($E_g/2 \sim 0.85\,\mathrm{eV}$) and up to the edge of the mid-IR region $\sim 2.15\,\mu$m. To access sufficiently high powers, for these measurements we only employed the femtosecond OPO. Furthermore, to minimize the effects of dispersion on the short pulses, we used a short piece of fiber ($L = 0.47\,\mathrm{cm}$) that was cut off during the characterization of the linear losses, which was considerably shorter than the dispersion length for all wavelengths ($L_\mathrm{D} \sim 1.44\,\mathrm{cm}$ at $1.55\,\mu$m). This allows for the neglect of dispersion during the propagation so that we can simply model the temporal evolution of the intensity profile under the influence of linear and nonlinear loss as [4]:

$$\frac{dI(z,t)}{dz} = -\alpha_l I(z,t) - \beta_\mathrm{TPA} I^2(z,t) - \sigma N_c(z,t) I(z,t), \tag{3}$$

where $I(z,t) = |A(z,t)|^2/A_\mathrm{eff}$, and $N_c$ is still determined via Eq. (2). The use of this simplified equation for the 200 fs pulses has been verified through a comparison with results obtained with a $\sim 1\,\mathrm{ps}$ (FWHM) telecoms fiber laser at $1.54\,\mu$m.

For each wavelength, the output power was recorded as a function of coupled input peak power and the results are plotted in Fig. 2(a). For all wavelengths there is a linear dependence on the output power for low input powers $< 50\,\mathrm{W}$. However, at higher input powers, the data for the short wavelengths (i.e., $1.55\,\mu$m and $1.65\,\mu$m) begin to saturate due to nonlinear absorption. In contrast, the largely linear trend exhibited for the longer wavelengths indicates that TPA is essentially negligible in this regime. As a result, this data provides an indication of the TPA edge of our core material, which is likely to be in the region $1.7\,\mu$m, or $E_g \sim 1.4-1.5\,\mathrm{eV}$. We note that a similarly low value of the bandgap energy of a-Si:H has been measured via ellipsometry in Ref. [3], and could be attributed to a change in material density due to the hydrogen content.

To establish the values of $\beta_\mathrm{TPA}$ for each wavelength, we fit the experimental data by numerically solving the coupled equations (2) and (3), with the linear losses given in Fig. 1(b). In this

#188410 - $15.00 USD Received 5 Apr 2013; revised 3 May 2013; accepted 13 May 2013; published 21 May 2013

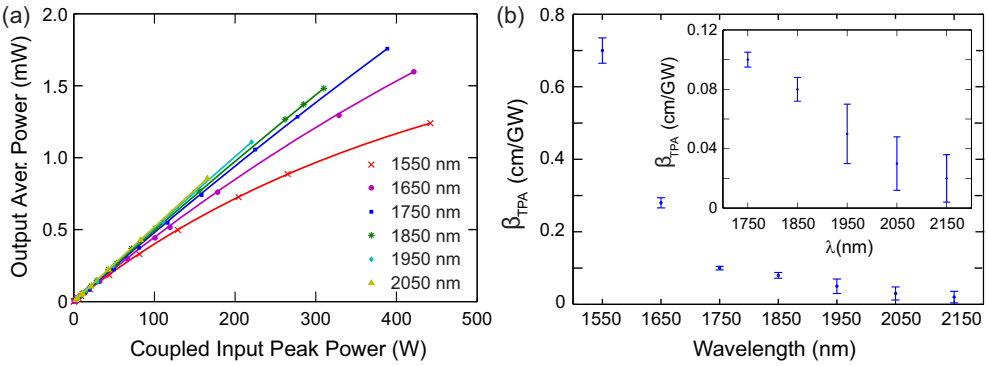


Fig. 2. (a) Nonlinear absorption measurements for the wavelengths given in the legend. The solid curves are the simulated fits obtained via solving Eqs. (2) and (3) for the corresponding wavelength. (b) TPA parameter as a function of wavelength extracted from Fig. 2(a). Inset: close up of the low value $\beta_{\mathrm{TPA}}$ region. Error bars represent the uncertainty in the input powers.

analysis we use $\tau_c \sim 100\,\mathrm{ns}$, as determined via pump-probe measurements [6], $A_{\mathrm{eff}} = 13\,\mu\mathrm{m}^2$, which has been estimated from modal analysis and shown to be approximately constant over the entire wavelength range [4], and $\sigma(\lambda)$, as calculated via the Drude model using the parameters for a-Si:H in Ref. [1]. The corresponding values obtained for the TPA parameter are plotted in Fig. 2(b) as a function of wavelength. These results show that $\beta_{\mathrm{TPA}}$ initially drops sharply from $0.70\,\mathrm{cm/GW}$ down to $0.28\,\mathrm{cm/GW}$ as the wavelength increases through the telecoms window ($1.55-1.65\,\mu\mathrm{m}$), then eventually begins to plateau at a negligible value of $0.05\,\mathrm{cm/GW}$ as the wavelength approaches the mid-IR regime ($1.95-2.15\,\mu\mathrm{m}$). This trend of decreasing $\beta_{\mathrm{TPA}}$ is as we would expect for wavelengths near the TPA edge, and specifically, we would also expect this to drop to zero for photon energies smaller than $E_g/2$, where the sum of the energies of two photons is no longer sufficient to span the bandgap. Here we attribute the non-zero values of $\beta_{\mathrm{TPA}}$ at the longer wavelengths, beyond the estimated TPA edge, to the exponential Urbach tail that extends the absorption edge of disordered materials, so that some TPA exists below the half bandgap [23]. Furthermore, although the value of $\beta_{\mathrm{TPA}}$ obtained at $1.55\,\mu\mathrm{m}$ is consistent with our previous reports in a-Si:H core fibers [6], as well as with other a-Si:H waveguides in the literature [3], as previously mentioned there is generally quite a variation in the measured TPA parameters for materials fabricated via different processes [2]. Thus, we anticipate that the position of the TPA edge may be tuned through the material deposition parameters to shift the region of low nonlinear loss to shorter wavelengths, and this is currently the subject of further investigations.

### *3.4. SPM induced spectral evolution*

To complete our characterizations, a series of experiments were conducted to study the spectral broadening induced by self-phase modulation (SPM) and determine the values of the Kerr coefficient $n_2$ over this wavelength range. As in the nonlinear absorption measurements, for these experiments we only used the high peak power femtosecond OPO for the input source, but this time we monitored the output via a long wavelength OSA (Yokogawa AQ6375) covering $1.2-2.4\,\mu\mathrm{m}$. The measured SPM spectra are shown in Fig. 3 over a selected range of input wavelengths from $1.55-2.15\,\mu\mathrm{m}$, for propagation over the complete $2.4\,\mathrm{cm}$ length. For each central wavelength, the output transmission spectra are recorded at two input peak powers, as designated by the legends. Here, the results obtained with low input powers are essentially

#188410 - $15.00 USD Received 5 Apr 2013; revised 3 May 2013; accepted 13 May 2013; published 21 May 2013

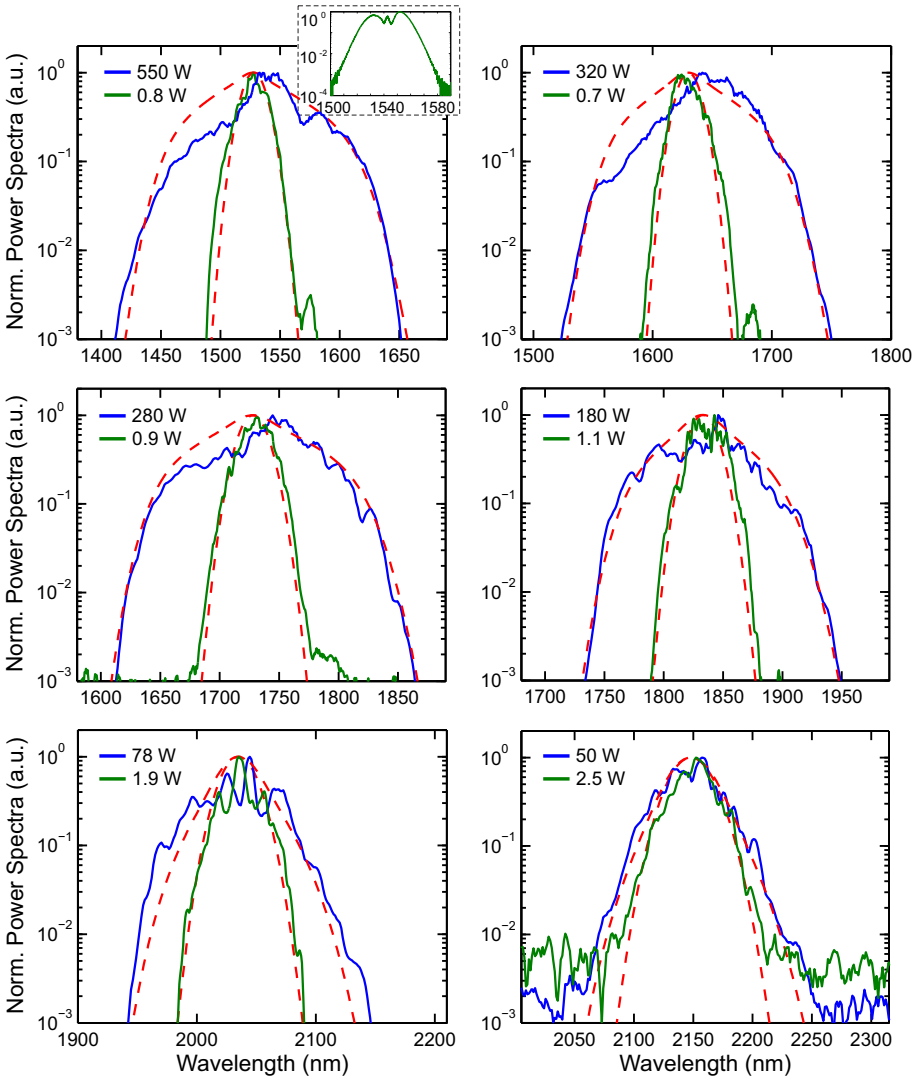


Fig. 3. Experimental power-dependent transmission spectra as a function of pump center wavelength, as labeled in the legends. The dashed lines are numerical fits obtained by solving Eqs. (1) and (2). Inset (top left): SPM spectrum generated in the a-Si:H core fiber using a $\sim 1$ ps fiber laser centered at 1.54 $\mu$m.

free from nonlinear propagation and are included as an indicator of the bandwidth of the input pulse, and thus as a means to determine the size of the initial negative frequency chirp on our pulses which are not transform-limited. The chirp was not found to vary dramatically over this wavelength range, and had a value of $C \sim -0.9$ at 1.55 $\mu$m for an input Gaussian of the form $A(0,t) = \sqrt{P_0}\exp[-1/2(1+iC)t^2/T_0^2]$, as determined from a comparison between the measured autocorrelation trace and a fit to the input spectrum which had a FWHM bandwidth of $\Delta\lambda \sim 23$ nm. The high power results are then used to illustrate the strong spectral broadening due to the large Kerr nonlinearity of the a-Si:H core material [4], with bandwidths of more than 200 nm obtained for all wavelengths below 2.05 $\mu$m. We attribute the limited spectral broadening seen for wavelengths above 2 $\mu$m to the increased coupling losses (from 0.6 dB at 1.55 $\mu$m

#188410 - $15.00 USD Received 5 Apr 2013; revised 3 May 2013; accepted 13 May 2013; published 21 May 2013

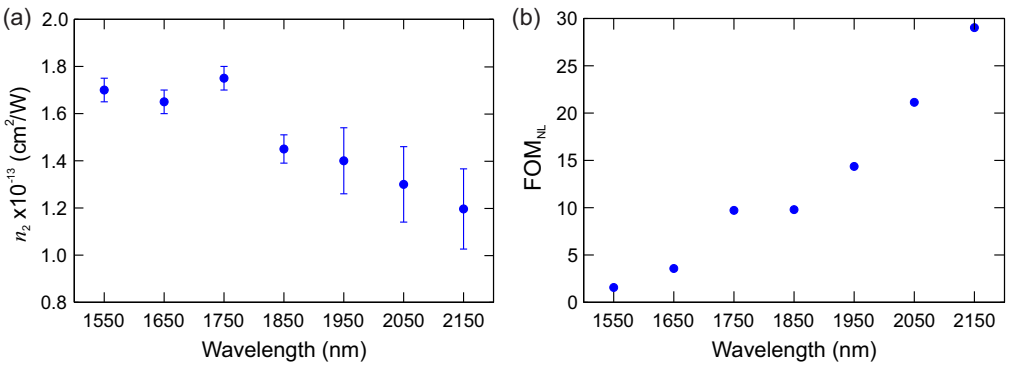


Fig. 4. (a) Wavelength dependence of the Kerr nonlinear coefficient $n_2$. Error bars represent the uncertainty in the input powers. (b) Wavelength dispersion of the $\mathrm{FOM_{NL}}$.

up to 3.8 dB at 2.1 $\mu$m) and the lack of output power as we move towards the edge of the tuning range of the OPO, and would expect to see proportionally larger bandwidths for 'hundreds of watts' input powers as used for the shorter wavelength measurements. It is also worth noting that the lack of clear SPM induced modulation on these spectra is in part due to the initial chirp and the noise on the input OPO spectra, but also due to the strong dispersion experienced by the femtosecond pulses. For comparison, the inset in the top left-hand corner of Fig. 3 shows the corresponding spectral broadening generated using the $\sim 1$ ps (FWHM) telecoms fiber laser, where the classic SPM shaping can be clearly observed.

The size of the Kerr coefficient for each central wavelength can then be established by fitting the spectral broadening with the solutions to Eqs. (1) and (2), obtained with the predetermined loss parameters. The corresponding values of $n_2$ are plotted in Fig. 4(a), which shows that as the input pulse wavelength is shifted across the TPA edge the $n_2$ value first increases slightly up to a value of $1.75\times10^{-13}\,\mathrm{cm^2/W}$ at 1.75 $\mu$m, then drops to a modest value of $1.2\times10^{-13}\,\mathrm{cm^2/W}$ at 2.15 $\mu$m. This trend is as we would expect from the nonlinear Kramers-Krönig relation, where the values of $n_2$ are expected to peak around the TPA edge, as similarly observed in c-Si around 2.2 $\mu$m ($E_g/2\sim0.56$ eV) [24]. We note that the larger error bars for longer wavelengths are due to the smaller broadening factors associated with the lack of available coupled power at these wavelengths.

As a final step, we have used our values of the nonlinear parameters $\beta_{\mathrm{TPA}}$ and $n_2$ to investigate the dispersion of the $\mathrm{FOM_{NL}}$, plotted in Fig. 4(b). This figure clearly shows that despite the decrease in $n_2$ at the longer wavelengths, the dramatic reduction in $\beta_{\mathrm{TPA}}$ results in a monotonic increase in the $\mathrm{FOM_{NL}}$. Thus, although the value of the $\mathrm{FOM_{NL}}$ at 1.55 $\mu$m for this a-Si:H core material is comparable to what we have reported before $\sim 1.6$, it increases rapidly to $\sim 10$ for the peak value of $n_2$ at 1.75 $\mu$m, then even further up to $\sim 28$ at the longest wavelengths. It is important to note that whilst the validity of this figure of merit could be questioned beyond the TPA edge, it has been applied to the long wavelengths based on the non-zero values of the TPA parameter, and provides a clear indicator of the advantage of moving into a regime of low nonlinear loss. Thus these results show that with a complete picture of the $\mathrm{FOM_{NL}}$ in the a-Si:H material, it is possible to access regimes of very highly nonlinear propagation, and thus it should be suitable for nonlinear applications around the 2 $\mu$m regime.

## 4. Conclusion

We have characterized both the linear and nonlinear transmission properties of our a-Si:H core fibers from telecoms wavelengths, across the TPA edge, and up to the edge of the mid-IR

#188410 - $15.00 USD Received 5 Apr 2013; revised 3 May 2013; accepted 13 May 2013; published 21 May 2013

regime. The dispersion curves obtained for the TPA and Kerr nonlinear parameters are in good qualitative agreement with the Kramers-Krönig transformations, and highlight the advantage of working in the vicinity of the TPA edge, where we have obtained some of the highest values of the $FOM_{NL}$ for this material to date. The results suggest that a-Si:H waveguides are a viable platform for nonlinear applications extending beyond telecoms, and into the short wavelength end of the mid-IR regime where applications include free-space communications, gas detection and medical diagnostics. We expect that continued efforts to understand the properties of this highly nonlinear material will help establish its use in wide ranging areas of research.

**Acknowledgments**

The authors acknowledge EPSRC (EP/G051755/1, EP/J004863/1, and EP/I035307/1), NSF (DMR-1107894) and the Penn State Materials Research Science and Engineering Center (NSF DMR-0820404) for financial support.

#188410 - $15.00 USD Received 5 Apr 2013; revised 3 May 2013; accepted 13 May 2013; published 21 May 2013